Supporting Information

Folker et al. 10.1073/pnas.1000824108

SI Materials and Methods

Reagents. Mouse and rabbit anti-FLAG antibodies were from Sigma, rabbit antipericentrin was from Covance, rat anti-tyrosinated tubulin (YL1/2) was prepared from hybridoma cells obtained from the European Collection of Cell Cultures, rabbit anti–nesprin-2G was prepared as described (1), MANLAC1 (mouse anti-lamin A) was from Glenn Morris (Wolfson Center for Inherited Neuromuscular Disease, Wrexham, United Kingdom), rabbit anti–β-catenin was from Invitrogen, and SUN2 antibody was from S. Shackleton (University of Leicester, Leicester, United Kingdom). Secondary antibodies absorbed to minimize cross-reactivity were purchased from Jackson ImmunoResearch Laboratories. Unless specified, all other reagents were from Sigma.

DNA Microinjection. Plasmid DNA was purified using a Plasmid Midi kit (Qiagen) and microinjected into nuclei of cells at the wound edge at 50 ng/μL in 10 mM Hepes (pH 7.4) and 150 mM KCl. For double injections, the two plasmids were simultaneously injected at 50 ng/μL each. Constructs were allowed to express for 4 h before stimulating centrosome orientation with LPA.

siRNA. Duplex siRNA (21-mers) was purchased from Shanghai GenePharma. The sequence used for lamin A was 5′ UUUAGGGUGAACUUCGGUGGG 3′ and that for GAPDH was 5′ AAAGUUGUCAUGGAUGACCTT 3′ as predicted by BIOPREDsi. Transfection with RNAiMAX was carried out using the reverse transfection protocol according to the manufacturer's instructions (Invitrogen). Efficiency of protein depletion was determined by Western blot analysis of total cell lysates.

Time-Lapse Microscopy. NIH 3T3 fibroblasts were grown to 80% confluency in 35-mm dishes with glass coverslip bottoms and then starved for 36–48 h in serum-free DMEM to generate a complete monolayer of quiescent cells. After wounding and expression of microinjected cDNAs, cells were washed twice with 2 mL of recording media [MEM amino acids (2.5 g/L glucose, 2 mM glutamine, 1 mM sodium pyruvate, 10 mM Hepes [pH 7.4]); GIBCO] and then transferred to a Nikon TE300 microscope and maintained at 37 °C with a heating chamber. Multiple fields were imaged using a motorized X-Y stage (Prior Scientific), and images were captured with either a 40× (1.0 N.A.) or 60× Planapo (1.4 N.A.) objective and a Coolsnap camera (Roper Scientific) controlled by Metamorph (Molecular Devices). Images for figures were assembled in Adobe Illustrator/Photoshop.

Analysis of TAN Lines. Movement of TAN lines and nuclei was analyzed using the track points function in Metamorph. Persistence was determined by measuring the time that an individual TAN line was present. Z-stacks were acquired at each time point to control for changes in focal plane.

Lamin A/C Incorporation. For the biochemical assay, NIH 3T3 fibroblasts were transfected using standard Lipofectamine transfection protocols (Invitrogen). One day after transfection, cells were lysed and extracted with 1% Triton X-100, 50 mM NaCl, and 50 mM Tris (pH 7.2) at 4 °C. Lysates were centrifuged at 12,000 × *g* for 30 min, and the supernatant was retained as the soluble fraction. The insoluble fraction was washed two times with lysis buffer and then resuspended and solubilized with SDS-sample buffer. Equal amounts of samples were then boiled and resolved by SDS/PAGE using 10% wt/vol gels, followed by transfer to nitrocellulose for Western blot analysis with a monoclonal antibody against the FLAG tag and a polyclonal antibody against vinculin as a loading control.

For confocal microscopy, DNA injection, cell fixation, and staining were the same as described for standard wide-field immunofluorescence. Imaging was performed on a Leica TCS LSI (Leica Microsystems). Image processing and analysis were performed using Velocity (PerkinElmer). Ratios of nuclear rim to nuclear interior staining were obtained by measuring the intensity across the diameter of the nucleus and dividing the intensity at the rim over the average intensity of the interior. Three individual focal planes were used for each nucleus to control for potential effects of the focal plane.

Quantification of Nesprin-2G Nuclear Levels. Fluorescence intensity of nuclei in cells that were immunofluorescently stained for nesprin-2G was measured using Metamorph after subtracting the background signal from an adjacent area of the coverslip without cells (2).

Statistics. In all experiments, a Student's *t* test was used to compare the experimental conditions with the control conditions. Tukey's posthoc analysis was performed to determine whether there were differences among the different groups of disease mutations. In all cases, the variants that cause muscle disease were separated into one group that was different from both the controls (uninjected and WT-expressing) and the variants that cause adipose disease. The variants that cause adipose disease were not distinguishable from control cells with respect to any measurement except for centrosome orientation (Fig. 1*B*) and centrosome position (Fig. 1*C*). Finally, by all measurements except centrosome orientation (Fig. 1*B*), the Tukey's posthoc analysis indicated that there are significant differences between each variant that causes muscle disease and each mutant that causes adipose disease with the exception of the discussed outliers, T528K and R482Q.

1. Patterson K, et al. (2004) The functions of Klarsicht and nuclear lamin in developmentally regulated nuclear migrations of photoreceptor cells in the Drosophila eye. *Mol Biol Cell* 15:600–610.

2. Gomes ER, Jani S, Gundersen GG (2005) Nuclear movement regulated by Cdc42, MRCK, myosin, and actin flow establishes MTOC polarization in migrating cells. *Cell* 121: 451–463.

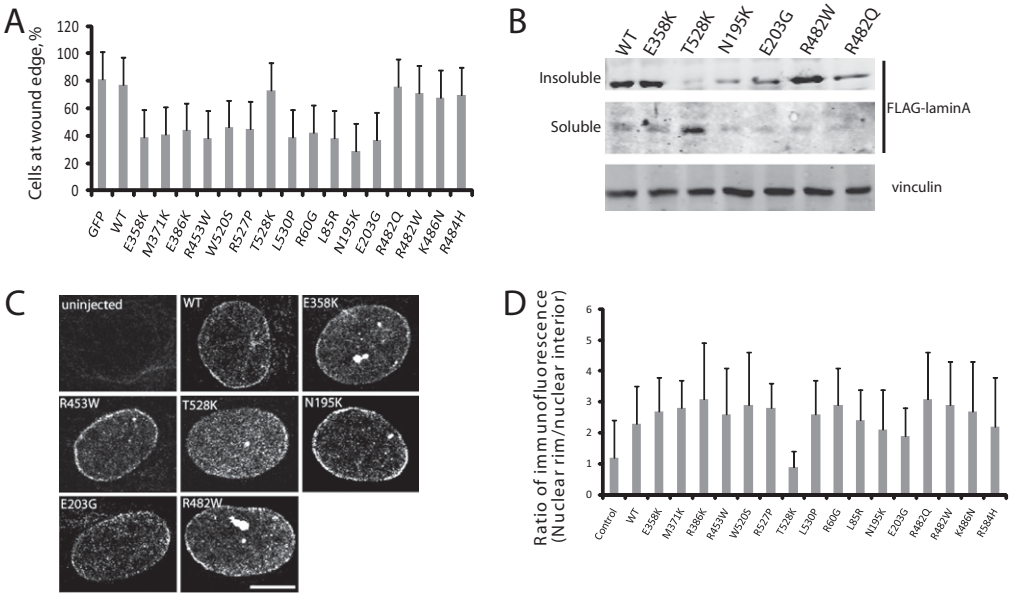

Fig. S1. (*A*) Percentage of NIH3T3 fibroblasts that express the indicated lamin A variants remaining at the wound edge after 24 h of migration in serum. The values for all EDMD variants (except T528K) were significantly different from GFP and WT control ($P < 0.05$). (*B*) Western blots of FLAG-tagged lamin A variants in Triton X-100 soluble and insoluble fractions of cell lysates. Vinculin is a loading control. (*C*) Confocal images (single planes) of immunofluorescently stained FLAG-tagged lamin A variants expressed for 4 h in NIH3T3 fibroblasts after DNA microinjection. Aggregates of some of the lamin A variants were observed but were not correlated with phenotypes. (*D*) FLAG-lamin A immunofluorescence intensity at the nuclear rim compared with the nuclear interior from images described in *C*. Error bars are SEM for >20 nuclei for each lamin A variant. Only the T528K variant was significant different ($P < 0.05$) from WT.

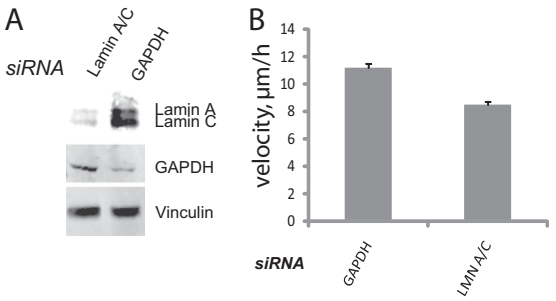

Fig. S2. (*A*) Western blots of lamin A/C and GAPDH in NIH3T3 fibroblasts depleted of the indicated proteins by siRNA. Vinculin is a loading control. (*B*) Velocity of NIH3T3 fibroblast migration into wounds following depletion of either GAPDH or lamin A/C by siRNA. Error bars are SEM from three individual experiments and velocities measured from 30 wound edges. Velocity is significantly different, $P < 0.05$.

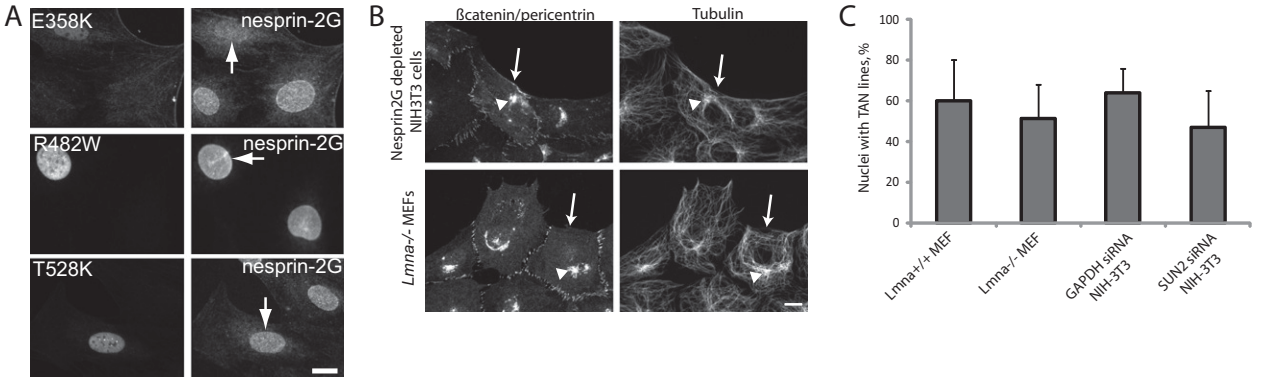

Fig. S3. (*A*) Immunofluorescence images of nesprin-2G in NIH3T3 fibroblasts expressing lamin A variants. Arrows indicate the expressing cells. (Scale bar, 10 µm.) (*B*) Immunofluorescence images of b-catenin/pericentrin and tubulin in nesprin-2G depleted NIH3T3 fibroblasts and *Lmna*$^{-/-}$ MEFs expressing GFP-mini-nesprin-2G (arrows indicate expressing cells; arrowheads indicate the centrosome). (Scale bar, 10 µm.) (*C*) Percentage of cells forming GFP-mini-nesprin-2G TAN lines upon expression of GFP-mini-nesprin-2G. Error bars are SEM for >40 cells from three independent experiments; differences are not significant ($P > 0.05$).